

The relevance of light in the formation of colloidal metal nanoparticles

Marek Grzelczak and Luis M. Liz-Marzán*

Corresponding author: mgrzelczak@cicbiomagune.es

This document is the Accepted Manuscript version of a Published Work that appeared in final form in Chem Soc Rev, copyright © Royal Society of Chemistry after peer review and technical editing by the publisher. To access the final edited and published work see *Chem. Soc. Rev.*, 2014, 43, 2089-2097. DOI: [10.1039/C3CS60256G](https://doi.org/10.1039/C3CS60256G)

The relevance of light in the formation of colloidal metal nanoparticles

Marek Grzelczak^{*a,b} and Luis M. Liz-Marzán^{a,b}

Received (in XXX, XXX) Xth XXXXXXXXXX 20XX, Accepted Xth XXXXXXXXXX 20XX

DOI: 10.1039/b000000x

5 “The possibility of using colloidal silver and gold as condensers for electron storage in artificial
photosynthesis has prompted the recent renewed interest in these areas.” This statement by Fendler and
co-workers in 1983 is even more relevant in today’s science and technology. In this *tutorial review* we
summarize research regarding the use of light in the synthesis of metallic nanoparticles. We describe how
light of different energies induces a variety of chemical events that culminate in the nucleation and
10 growth of metal nanocrystals. Light can thus be used as a handle to direct metal nanocrystal growth and
improve tunability and reproducibility.

Introduction

Light is a ubiquitous component, though often neglected, in
chemical synthesis. The increasing attention toward the use of
15 light in the synthesis of nanoparticles is due to the technological
and scientific interest in making use of inexpensive solar energy.
In the field of colloid chemistry, light remains an exotic tool that
might be used to control particle shape, size and composition.
Light assisted synthesis, as compared to standard chemical
20 approaches, provides the advantages of a uniform distribution of
the reducing agent in the entire solution, easy modulation of the
power density, and tuning of the wavelength to maximize the
absorption by chemical species in solution.

Light is of particular relevance in the field of plasmonics, in
25 which materials interact strongly with the incoming radiation.
Therefore, the use of light in the synthesis of plasmonic
nanoparticles may represent a double benefit, since nanoparticles
provide a colorimetric signal that may assist in retrieving
mechanistic insights on the photochemical processes occurring in
30 solution. In the past, the kinetics of nanoparticle formation have
provided important information on photochemical pathways.
Within this line, progressive understanding of the chemical
processes taking place in the presence of light, offers new
synthetic tools for manipulation of light induced particle
35 nucleation and growth, with a relatively high level of control.
Thus, proper understanding of the physics behind light-particle
interactions will confer plasmonic nanoparticles a central spot in
chemical processing, since they provide synthetic tools that can
be largely exploited in fields such as organic chemistry or
40 catalysis.

In this tutorial review we discuss the role of light in the, wet-
chemical synthesis of metallic nanoparticles and how it affects
the current synthetic models on nucleation and growth of such
metal nanoparticles. Although we are aware of the works devoted
45 to synthesis of non-noble metal nanoparticles in the presence of
light, we limited our discussion mostly to plasmonic
nanoparticles. Interested readers will find exhaustive information
on non-noble particles in a recently published review.¹ Our

discussion culminates with the proposal of new synthetic models
50 for more efficient and versatile fabrication of nanoparticles using
light as energy input.

Nucleation and Growth vs. Autocatalysis

Wet chemical approaches for metal nanoparticles synthesis
may be classified according to two major mechanisms:
55 nucleation/growth and autocatalytic reduction, so-called seeded-
growth (see Figure 1). Historically, the former model was
exploited by Faraday to prepare solutions containing “finely
dispersed metals”. In this approach, a metal salt is reduced by a
strong reducing agent to produce dispersed nanoparticles.
60 Organic molecules present in solution adsorb onto the surface of
the newly formed particles, providing colloidal stability and thus
preventing sedimentation. Subsequent advancements by
Turkevich and Frens allowed additional control on the size of the
particles, through the molar ratio between stabilizing/reducing
65 agent and metal precursor.² By that time, LaMer proposed a
general model for the synthesis of monodispersed colloids.³
Although initially proposed for colloidal sulfur, the model found
general acceptance in the synthesis of noble metal-based sols.
Briefly, to obtain monodispersed particles one should increase the
70 nucleation rate so that after the first nucleation burst no additional
nuclei are formed and a saturation point is reached at which
individual precursors only deposit on existing particles – the
growth process. Since the saturation point is achieved faster at
high concentration of the metal precursor, this approach permits
75 the synthesis of large amounts of particles without loss of quality.
Interestingly, the fast kinetics of the process may indeed provide
monodispersity, but at the expense of forming particles with
energetically favorable shapes – isotropic.

However, anisotropic particles have become particularly
80 attractive because their decreased symmetry often leads to
unusual chemical and physical behavior. Thus, more exotic
shapes bring complexity to the optical response, which has been
shown to be crucial toward important technological developments
(e.g. 3D plasmonic rulers or metamaterials with negative
85 refractive index). Therefore, the need for synthetic approaches

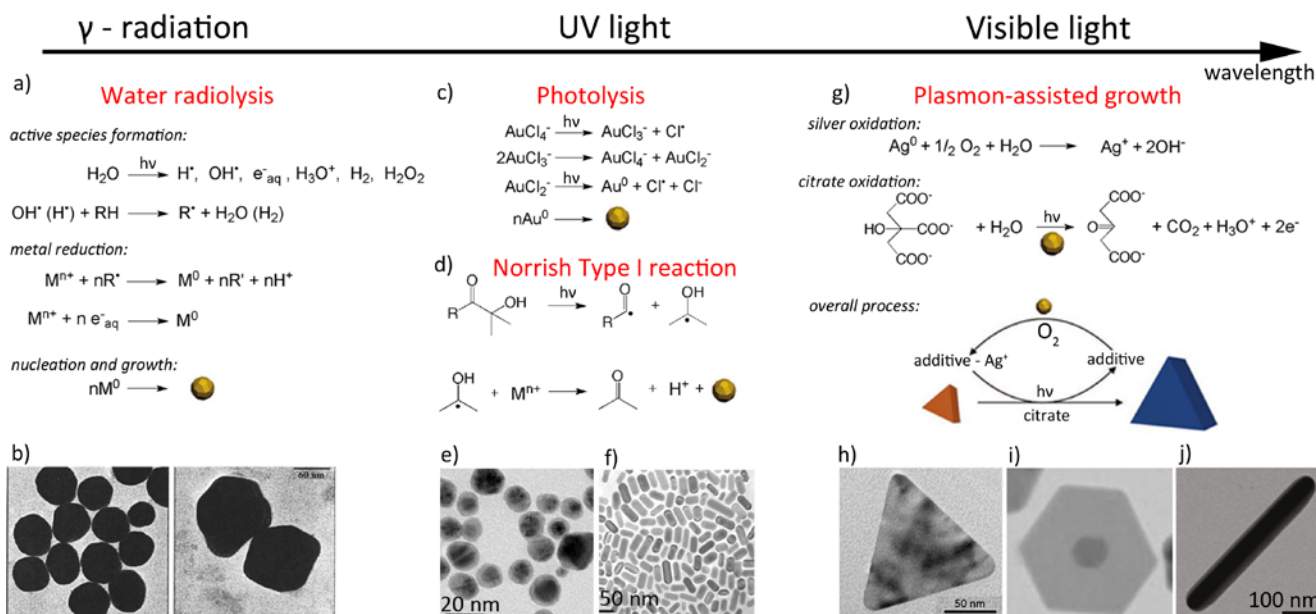


Fig.2 Synthesis of nanoparticles in the presence of light. Electromagnetic radiations of different wavelengths induce a variety of chemical events that induce nucleation and growth of metallic nanoparticles. (a-b) Synthesis by γ -radiation. (a) Chemical pathway to generate energetic species (radicals and hydrated electrons), which in turn reduce metal ions to produce stable colloids. (b) Example of colloidal gold prepared via γ -radiation with controllable sizes. (c-f) UV light –assisted synthesis of metallic nanoparticles. (c) Photolysis of a metal precursor under UV radiation leads to formation metal nuclei and further growth of the particles. (d) Generated ketyl radicals via Norrish type I cleavage can rapidly reduce a metal precursor. (e) Au@Ag core/shell nanoparticles prepared within the scope of the seeded-growth model. (f) Photochemically produced gold nanorods in the presence of Ag^+ (g-j) Plasmon assisted synthesis of nanoparticles under visible light irradiation. (g) Oxidative formation of silver precursor from Ag seeds and electron donation from citrate ions lead to formation of silver nanoparticles under visible light. (h) Silver triangles. (i) Au@Ag core/shell. (j) Silver nanorods prepared from Ag seeds. Figures (b), (e), (f), (h), (i), (j) reproduced with permission from refs. 18, 25, 29, 35, 40, 39, respectively.

γ - radiation

The irradiation of an aqueous solution of chloroauric acid with γ -rays from a ^{60}Co source produces colloidal gold particles with 80 nm of diameter. Such photochemical gold nanoparticle synthesis was first reported by Fujita and et al.¹¹ Later works by Henglein, Fendler and Belloni established methodologies and mechanisms for the synthesis of gold,^{12–15} silver¹⁶ and copper¹⁷ nanoparticles with different sizes.¹⁸ Typical radiolytic syntheses of metal nanoparticles involve the radiolysis of water, in which hydrated electrons and hydroxyl radicals are generated by electrons created by means of a Van de Graaf generator. The hydroxyl radicals from the radiolysis of water rapidly react with alcohol to produce hydroxyalkyl radicals. These species can react with the molecules in solution yielding new radicals capable of reducing the metal precursor into the zero-valent state (Figure 2a). Although the energy input during the process is relatively high (MeV), the nucleation step is relatively slow because of numerous chemical transitions taking place prior to the formation of metallic clusters. The nucleation process, however, can be modulated through various parameters, such as the chemical nature of the radical scavengers, the presence of gases, or even by pH.¹² A major advantage of this method is that the reducing agent is uniformly generated in solution and the reaction rate is controlled by the number of reducing equivalents generated by the irradiation. As a result, nearly monodispersed particles are formed since a large number of atoms is homogeneously produced during the irradiation. Interestingly, the radiolysis protocol was also extended to the seed-mediated growth of gold nanoparticles with

precise control over the final particle size.^{18,13} Conventional citrate-stabilized gold nanoparticles were enlarged upon mild reduction of $\text{Au}(\text{CN})_2$ by radiolytically generated hydroxymethyl radicals.¹⁸ The radicals donate an electron to the seed particles which then selectively reduce Au ions on the metal surface. The enlargement process yielded particles up to a maximum diameter of 120 nm (Figure 2b). This protocol was also extended to produce core-shell nanoparticles consisting of silver cores and gold shells,¹⁹ which are particularly difficult to obtain through other methods because of Galvanic replacement reactions.

Despite all the benefits of the water radiolysis method, the requirement of a strong energy input to commence the nucleation of metal nanoparticles pinpointed the need of using a light source with lower energy. UV was quickly seen as a straightforward choice and there are plenty of published reports regarding the synthesis of metallic nanoparticles under UV-irradiation. Therefore, we only focus here on selected relevant approaches.

UV irradiation

The weak photostability of transition metal complexes under UV illumination induces a gradual dissociation of the metal ions from the complex to produce stable metal clusters or colloids.²⁰ For instance, irradiation of AuCl_4^- solution with 253.7 nm light induces the photolysis of the complex to produce atomic Au^0 , which coagulates into colloidal gold (Figure 2c).²¹ In the case of silver, excited Ag^+ from AgClO_4 can oxidize H_2O resulting in the formation of silver atoms and subsequent agglomeration to produce colloidal silver.²¹ Therefore, photolysis of the metal precursor in the presence of UV light becomes a synthetic tool for

the synthesis of plasmonic nanoparticles.^{14,21,22}

Photoreduction of a metal precursor in the presence of ligand molecules, such as polymers, provides additional control over the size and shape of the nanoparticles. Huang et al. proposed the UV photoreduction of silver nitrate in the presence of poly(N-vinylpyrrolidone) (PVP). The presence of PVP affected the diameter of the final nanoparticles and the rate of metal photoreduction. Increasing the amount of PVP (0.25 -1 wt%) was found to decrease the particle diameter (22-15 nm), along with a faster rate of the photochemical process. The authors proposed that PVP is directly involved in the photochemical process. As PVP contains carbonyl groups that absorb UV light, excited species could reduce Ag^+ to Ag^0 . Alternatively, excited Ag^+ could oxidize carbonyl groups from PVP into carboxylic acid. In another work, polyvinyl alcohol (PVA) and polyethylene glycol (PEG) were used as capping agents in the photochemical synthesis of gold nanoparticles with various shapes. Upon extended UV irradiation (48 h) of an aqueous solution containing PVA and HAuCl_4 mostly plate-like nanoparticles were obtained. Au nanoparticles with quasi-ellipsoidal morphology were obtained using PEG instead of PVA as polymer capping agent. Although the authors omitted a mechanistic analysis of this process, it seems obvious that light, as a reducing agent, can induce significant changes in the reaction mixture to facilitate nucleation and growth of the particles with different morphologies.

Colloidal nanofabrication has also profited from advancements in the field of polymer science. A large number of photoinitiators, commonly used in photopolymerization processes, can be applied in the nucleation and growth of metallic nanoparticles. Scaiano's group significantly contributed to this field by using commercial photoinitiators that induce nucleation of gold²³ or silver²⁴ nanoparticles under UV irradiation. The advantage of this method is that the chemistry involved is well known. All these syntheses are initiated by Norrish type I cleavage reactions, in which UV light cleaves one of the C-C bonds from aliphatic or aromatic ketones, producing strongly reducing free radicals (Figure 2d).¹ Therefore, the stoichiometric relation between the photoinitiator and the metal precursors yields monodisperse nanoparticles within few minutes of UV irradiation. Additionally, substoichiometric amounts of photoinitiator allow the implementation of this reaction for seeded-growth of gold nanoparticles.²⁵ Preformed nanoparticle seeds can store electrons from decomposed molecules facilitating gradual reduction of the metal salt on the surface of the seeds. Apart from the size control of the final particles, the composition was also controlled in Au@Ag core@shell structures (Figure 2e).²⁶ A major disadvantage, however, is the need of using hydroxylic solvents (e.g water, alcohols). The cleavage of the C-C bond releases an electron and a proton, which need to be captured by the metal complex and solvent molecules, respectively. Thus, the synthesis of particles by Norrish type I reactions failed in solvents that are unable to accept protons (e.g THF or toluene).¹

Cationic surfactants are another class of molecules that are suitable for photochemical synthesis of nanoparticles. Esumi and coworkers found that complexes between AuCl_4^- and cationic surfactants are suitable precursors for the synthesis of gold

nanoparticles under UV irradiation.²⁷ They found that prior to metal nucleation the complex between surfactant and metal precursor undergoes photolysis, accompanied by oxidation of the surfactant molecules. Importantly, the size of the nanoparticles could be tuned through the concentration of the surfactant in the mixture, so that increasing concentrations led to a decrease in the final particle diameter. In later studies by the same group, gold nanorods/nanowires were obtained under UV light irradiation at high cationic surfactant (C_nTAC – cetyltrimethylammonium chloride) concentrations.²⁸ Although the source of electrons in the photochemical process was not identified and the yield of anisotropic nanoparticles was low, the importance of using a surfactant in the synthesis of anisotropic nanoparticles was again confirmed.

The important breakthrough in the photochemical synthesis of gold nanorods was achieved by Yang and co-workers,²⁹ who used CTAB – (cetyltrimethylammonium bromide) as a capping agent in the presence of acetone (Figure 2f). The presence of silver nitrate in the growth solution (no seeds) was found to be crucial to obtain gold nanorods. In fact, the amount of Ag^+ dictated the final aspect ratio of the gold nanorods, which varied from 1 to 5. The authors proposed that Br^- form CTAB and Ag^+ ions could produce insoluble AgBr crystals that under UV light irradiation were reduced to Ag nanoclusters. These Ag clusters were later oxidized back to AgBr facilitating the formation of gold nanorods. In a latter work by Placido et al. the mechanism of photochemical formation of gold nanorods was investigated.³⁰ UV irradiation was proposed to decompose acetone to produce ketyl radicals, which in turn remove hydrogen atoms from CTAB molecules. Such alkyl radicals generated from CTAB can reduce Au(III) into Au seeds. Subsequently, the Au seeds catalyze the reduction of Ag^+ into tiny Ag clusters, which are finally reoxidized in the presence of Au(I), which is being incorporated into the crystalline lattice. The well-established underpotential deposition (UPD) model was used to explain the symmetry breaking required for gold nanorod formation. During the growth, Ag(0) adsorbs strongly onto the lateral facets possessing higher surface energy, whereas the adsorption of Ag(0) on the tips is weaker, due to a lower surface energy, facilitating higher silver reduction/oxidation rate and thereby increasing the rate of gold reduction along the long axis.

Visible light

Since the localized surface plasmon resonance (LSPR) frequencies of metal nanoparticles can be tuned within the visible and NIR spectral ranges, incident light of these particular wavelengths has gained special relevance in the synthesis of noble metal nanoparticles. The most representative example is probably the photoinduced formation of silver nanoprisms from small silver spheres, in the presence of citrate ions.³² Mirkin et al. showed that the process is driven by surface plasmon excitations, in which the incident illumination wavelength overlaps with the LSPR of newly formed nanoprisms. As the position of the LSPR is directly related to the particle size, this method allows size control simply by selecting the appropriate incident wavelength. In subsequent works by the same and other groups, a three-step growth mechanism was proposed (Figure 2g).³³ First, the preformed Ag seeds get partially oxidized by dissolved O_2 to

produce free Ag^+ in the solution. Light absorption by the same seeds induces plasmon oscillations, which upon decay generate highly energetic “hot” holes that oxidize citrate ions adsorbed on the particle surface. Stored electrons in the seed nanoparticles autocatalytically reduce silver ions on their surface promoting a gradual increase of particle size. The final shape of the nanoparticles is defined by site-specific plasmon excitation that induces face-selective Ag^+ reduction. It has been found that the rate of silver reduction is crucial to control the growth process.³⁴

Through the dynamic oxidation and reduction of silver ions, the concentration of the metal precursor remains constant. However, the presence of additives, such as bis(*p*-sulfonatophenyl)phenylphosphine dipotassium salt (BSPP)³⁴ or PVP³⁵ increases the solubility of the precursor by formation of complexes, thereby increasing the rate of metal reduction. By tuning the experimental conditions (e.g. silver reduction rate or pH), particles with different shapes and composition were proposed, such as tetrahedra,³⁶ decahedra,³⁷ icosahedra,³⁸ nanorods,³⁹ or Au@Ag core-shell structures⁴⁰ (for some examples see Figure 2 h-j).

From a general perspective, this reaction model reminds us of a typical photocatalytic process in which a photosensitizer (here the plasmonic nanoparticles) absorbs light and then directs an electron flow from the electron donor (citrate ions) to an electron acceptor (Ag^+), giving rise to the formation of nanocrystals. It is then straightforward that plasmon-mediated synthesis will be soon extrapolated for the fabrication of particles with different metal compositions. In fact, recent example on light harvesting by plasmonic nanoparticles to induce chemical reactions⁴¹ confirms the potential of plasmon resonances in the light-assisted synthesis of nanoparticles.

One can note that with increasing the wavelength – or decreasing the energy - of the incident light, the anisotropy of the final nanoparticle products increases (Figure 2). This is directly related to the chemical nature and physical properties of the intermediate products that induce metal reduction. Under γ -radiation, highly energetic hydrated electrons with lifetimes of the order of microseconds ensure fast nucleation of the metal ions. As a result, mostly spherical particles are formed. In UV light assisted synthesis, ketyl radicals with millisecond lifetimes enhance the probability of metal ions reduction over longer timescales, thereby opening the possibility to modulate particle shape. Plasmon-assisted nucleation under visible light is a relatively slow process. Because metallic nanoparticles can easily retain photogenerated electrons, the induction time is often detected before the reduction commences. This delay can be an advantage if one seeks for shape modulation.

Laser ablation synthesis

The use of pulse laser light with visible or near-IR wavelengths can be used to produce metallic nanoparticles from bulk precursors. In so-called laser ablation methods, the nanosecond pulse laser beam with high energy density (10^8 – 10^{10} W cm^{-2}) heat the metal target to generate plasma, vapor and metal nanosized droplets, which further react with the liquid medium to form nanoparticles.³¹ The main difference from conventional synthesis is that practically any kind of particles can be prepared from any base material (e.g. metal, alloy, ceramic). As the final size of the particles is hardly affected by laser parameters, a

quenching method has been proposed to control the dimensions of the nanoparticles. For example, by addition of molecular quenchers (surfactant, DNA, proteins) at different concentrations, the particle size could be controlled in the range from 5 to 50 nm. The main advantage of the laser ablation method is the possibility to fabricate ligand-free colloids with accessible surface, rendering them attractive materials for catalytic and biosensing applications.

Light-assisted nucleation on templates

As mentioned above, seeded-growth is based on the autocatalytic reduction of metal ions on the surface of preformed seeds. A straightforward generalization of this model should allow the use of any materials that catalyze the reduction of metal nanoparticles on their surface. In fact, in the field of photocatalysis noble metals are used as electron scavengers, which can quantitatively indicate the performance of the photocatalyst. We list below a few examples in which the nucleation and growth of noble metal nanoparticles, rather than the photocatalytic activity are highlighted. In general, catalysts are classified by their chemical composition. Thus, we discuss nucleation of metal nanoparticles on (i) semiconducting oxides, quantum dots, carbon based nanostructures (carbon nanotubes and graphene), and supramolecular assemblies.

Photo-reduction of metals on the surface of oxides has been extensively studied for applications in catalysis. Bard and coworkers used platinumized TiO_2 powder for the photosynthetic production of amino acids under UV irradiation.⁴² Although the presence of Pt clusters was essential to initiate any chemical processes, the mechanism for platinum photoreduction on the semiconductor surface was fairly well understood. Later works by Kamat and colleagues provided significant understanding of the photochemical processes behind metal nucleation.⁴³ When a TiO_2 nanoparticle suspension in ethanol was subjected to UV irradiation, it turned blue as photogenerated electrons were trapped within TiO_2 at Ti^{4+} sites. While the holes are irreversibly scavenged by ethanol, the addition of Ag^+ results in the nucleation of the metal on the oxide surface. Interestingly, the number of electrons stored in the TiO_2 semiconductor can be easily quantified by monitoring the evolution of the plasmon band of newly formed nanoparticles. From an application standpoint, metallic nanocrystals play an important role in TiO_2 -Ag composites, as the metal can store electrons. Thus, under illumination the flow of electrons can be controlled, which is of great importance for the desired redox reactions to take place in solution. Nucleation of silver nanoparticles is particularly interesting in the presence of non-spherical TiO_2 particles. In the work by Cozzoli et al.⁴⁴ organic soluble TiO_2 nanorods ($30 \times 4 \text{ nm}^2$) acted as both catalyst and stabilizer of photochemically generated spherical silver nanoparticles (50 nm). Nucleation of metallic silver took place mostly on the tips, where the surfactant molecules were less coordinated as compared to the lateral facets (Figure 3a). During the growth of particles under UV light, the semiconductor nanorods progressively get organized around the silver particles, acting as an inorganic stabilizer. Precise control over the population and size of silver nanoparticles on the surface of TiO_2 nanorods ($50 \times 15 \text{ nm}^2$) was achieved by Dinh et al.⁴⁵ The population of Ag clusters on the surface of individual TiO_2

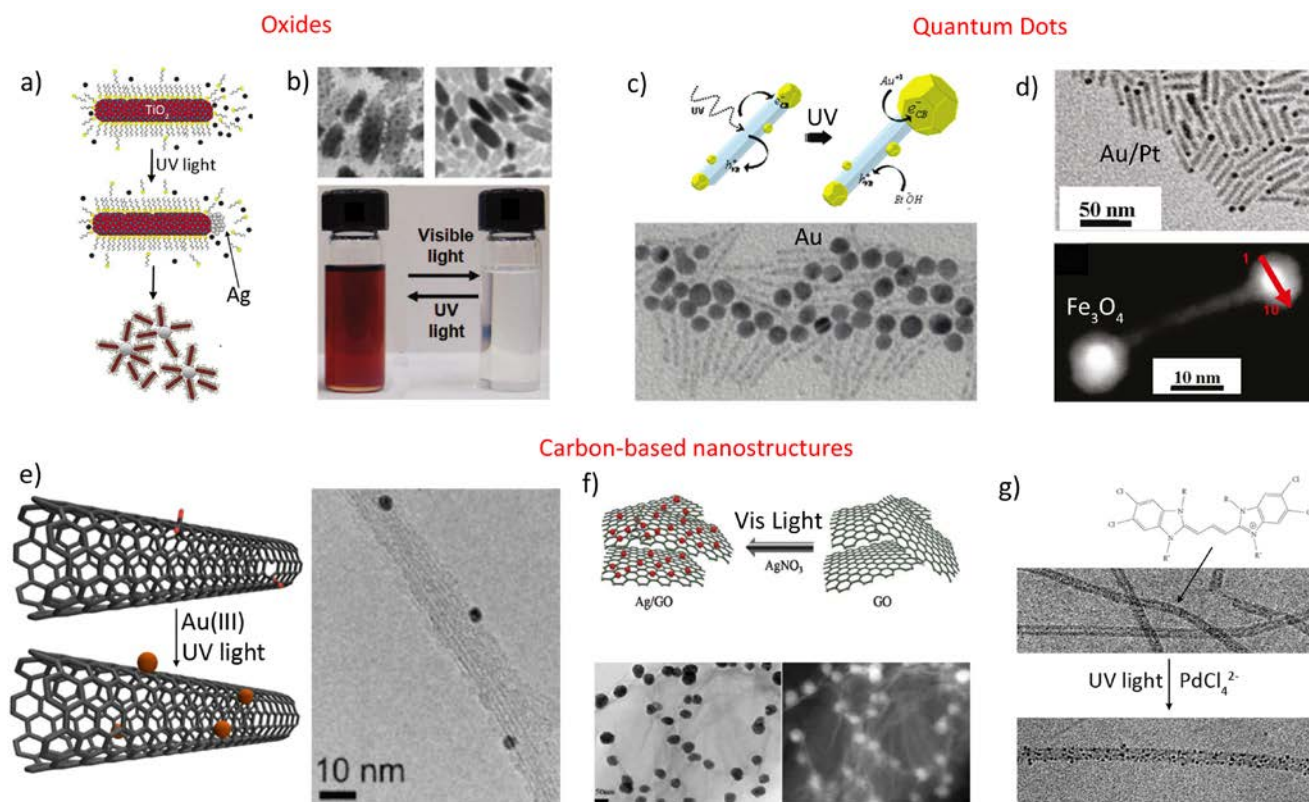


Fig.3 Light-assisted nucleation of nanoparticles on a template. (a-b) Oxide as a template. (a) Dual role of TiO₂ nanorods: photocatalyst and stabilizing agent. (b) Reversible photoreduction of Ag nanoparticles on TiO₂ rods. (c-d) Nucleation of metals on the surface of quantum dots. (c) Formation of Au nanoparticles on one tip of QD rods. (d) Photoreduction of Pt/Au and Fe₃O₄ nanoparticles on Au-QD rods. (e-g) Carbon-based nanostructures as templates (e) Selective reduction of Au nanoparticles on the surface of single walled carbon nanotubes. (f) Nucleation of Ag nanoparticles on graphene oxide. (g) Photoreduction of Pd nanoparticles on assembled organic dyes. Figures (a), (b), (c), (d), (e), (f), (g) reproduced with permission from refs. 44, 45, 47, 49, 50, 52, 54, respectively.

nanorods could be controlled by the amount of hydrophobic surfactant (oleic acid), which determines the number of nucleation points on the semiconductor surface. The size of the silver nanoclusters (2–3.5 nm) was altered by varying UV irradiation time (Figure 3b). Interestingly, a reversible color change of the hybrid TiO₂-Ag composite was induced by altering UV and visible light illumination. Exposition of the TiO₂-Ag composite to air under visible light resulted in silver oxidation, accompanied by disappearance of the characteristic LSPR band. Recovery of the initial color, as well as the number of silver clusters per TiO₂ nanorod was achieved by repeated UV irradiation cycles.

As shown above, the relatively large band gap of TiO₂ requires UV light to promote photoreduction of silver nanoparticles. Combination of TiO₂ with plasmonic nanoparticles has been recently used for the formation of metallic nanocrystals under visible light. For instance, Zhou et al.⁴⁶ have shown that Au_{rod}@TiO₂ core@shell nanoparticles can induce silver nucleation on the oxide surface under visible light irradiation at 633 nm, which matches the longitudinal LSPR of the Au nanorod core. Under visible light irradiation, generated hot electrons in the gold rods are transferred to the TiO₂ conduction band, and then scavenged by Ag⁺ to form silver nanoparticles (10 nm).

Quantum dots are also suitable for light-assisted nanoparticle nucleation. These semiconductor nanoparticles with size-

dependent band gap energy can efficiently emit light at practically any wavelength of the solar spectrum. Although fluorescence-related applications of these nanocrystals are well established, their use as photocatalysts have recently gained increasing attention. The possibility of converting the light energy into chemical bonds in the form metallic nanocrystals has been proposed.^{47,48} Upon UV irradiation, 15 nm gold domains were exclusively formed on one side of CdS nanorods (Figure 3c). Regarding the mechanism, upon addition of Au(III), small Au⁰ domains instantly form on the entire rod surface, even in the absence of light. Upon UV stimulation, the electrons created in the semiconductor migrate preferentially to one of the metal tips, further reducing Au(III), whereas a hole was reduced by the solvent. Interestingly, the process of gold domain formation could be observed at the single nanoparticle level by using dark field microspectroscopy. Au-tipped CdSe/CdS nanorods were later exploited for the transfer of electrons from CdS to the Au tips upon UV excitation, promoting selective metal deposition on the gold side.⁴⁹ The gold tip in this system has also served as a heterogeneous nucleation site for the deposition of different metals. For instance, Pd/Au alloyed tips were formed while preserving the rest of the semiconductor intact (Figure 3d). In the same work, successful photoreduction of iron under UV light was achieved selectively on the gold tips. Subsequent oxidation of the iron under aerobic conditions led to the formation of

semiconductor nanorods with iron oxide tips (Figure 3d), giving rise to heterogeneous nanostructures with magnetic and optical properties. Interestingly, the use of light during the formation of metal NPs on quantum rods leads to regioselective nucleation. While thermally induced techniques lead to formation of gold nanoparticles on the whole surface, light assisted methods result in metallic cluster growth exclusively on the tips.

Carbon-based nanomaterials, such as carbon nanotubes^{50,51} or graphene,^{52,53} were also exploited for the selective light-induced reduction of metal nanoparticles. In the work by Quintana et al.,⁵⁰ gold nanoclusters (2 nm) were synthesized on the surface of oxidized single walled carbon nanotubes (SWNT) (Figure 3e). The results indicate that oxidized defects at the sidewalls of SWNT played an important role as nucleation sites for the formation of metallic gold. The density of the formed gold nanoparticles was tuned by the number of oxidative defects in the SWNT skeleton. Interestingly, gold nucleation kinetics was found to depend on the electronic structure of the SWNT, with faster nucleation observed on metallic SWNT, which was associated with a higher probability of electron-hole pair formation on this type of nanotubes. The photoactivity of graphene oxide (GO) in the visible spectral range renders it an attractive photocatalyst to induce metal reduction with no need of using highly energetic radiations. Moon et al.⁵² showed that visible light irradiation, above 420 nm, induced the formation of silver and gold nanoparticles on graphene oxide sheets without chemical reducing agents (Figure 3f). Electron transfer between the metal ions and GO – here an electron donor –, mediated the metal reduction. In analogy to carbon nanotubes, oxidized defects in GO played an important role in the nucleation process, providing a platform for the homogenous distribution of metal centers on the carbon-based nanosheets.

The above examples show that the major part of the studied photocatalysts are solid nanometric structures that can absorb light, which is later stored in chemical bonds through metal reduction. However, supramolecular architectures consisting of small molecules (often dyes) can also play the role of a template or a photocatalyst to induce selective metal reduction on their surface. For example, one-dimensional tubular aggregates of tetrachlorobenzimidacarbocyanine dye can mediate the formation of silver or palladium nanoparticles via a photo-induced electron transfer process (Figure 3g).⁵⁴ In the presence of light, the molecular building blocks can be partially oxidized, promoting metal reduction. These examples show that the combination of supramolecular, colloid and photo-chemistry can be successfully implemented for the synthesis of hierarchical and dynamic assemblies with multiple functionalities.

Conclusions

Although control over the quality of nanoparticles has not been fully developed in light-assisted syntheses, future advances and better understanding of chemical processes will surely bring attractive synthetic solutions in colloidal fabrication. Today, when colloid-based nanomaterials progressively gain importance in everyday applications (e.g. sensing), their possible use in developing countries is also relevant. Thus, easy access to sunlight at any point of our planet makes it very attractive the use

of light to control the growth of nanocrystals, not only with perspectives for biosensing, but also for energy storage in chemical bonds and subsequent release for further reactions.

The two main mechanisms involved in nanoparticle formation, namely nucleation and seed-assisted growth (with or without light), offer enormous synthetic versatility in colloidal nanofabrication. Particle size, shape and composition can be easily designed and tailored. However, for the sake of sustainability in colloidal chemistry both synthetic models should be combined, so that nanoparticle seeds would catalyze the nucleation and growth of the other nanoparticles, but within the rules of the seeded-growth model. That is, the seeds will determine the size and shape of the newly formed nanoparticles. As we have shown, light can be an extremely useful and versatile synthetic factor to control such processes. In fact, a recent work by Grzybowski and co-workers demonstrated that such a synthetic approach is indeed feasible.⁵⁵ They showed that nanoparticles comprising Fe₂O₃ and Pd domains can act as efficient photocatalysts, driving the photoreduction of metal salts into colloidally stable metal nanoparticles. Although this is just an example to be added to those discussed above, it shows that the interaction of light with metallic nanostructures can still offer a large number of uses and applications, not only to optimized the synthetic protocols but also to design working devices.

Acknowledgments

Funding is acknowledged from the European Research Council (PLASMAQUO, 267867). M.G. acknowledges the receipt of a fellowship from IKERBASQUE, the Basque Foundation for Science.

Notes and references

^a BioNanoPlasmonics Laboratory, CIC biomaGUNE, Paseo de Miramón 182, 20009 Donostia – San Sebastián, Spain. Fax: +34 943 005 301; Tel: +34 943 005 300; E-mail: mgrzelczak@cicbiomagune.es
^b Ikerbasque, Basque Foundation for Science, Bilbao, Spain.

1. J. C. Scaiano, K. G. Stamplecoskie, and G. L. Hallett-Tapley, *Chem. Commun.*, 2012, **48**, 4798–4808.
2. G. Frens, *Nature*, 1973, **241**, 20–22.
3. V. K. LaMer and R. H. Dinegar, *J. Am. Chem. Soc.*, 1950, **72**, 4847–4854.
4. J. Turkevich, P. C. Stevenson, and J. Hillier, *Discuss. Faraday Soc.*, 1951, **11**, 55–75.
5. J. Turkevich, *Gold Bull*, 1985, **18**, 86–91.
6. C. Lofton and W. Sigmund, *Adv. Funct. Mater.*, 2005, **15**, 1197–1208.
7. G. Wang, T. Nishio, M. Sato, A. Ishikawa, K. Nambara, K. Nagakawa, Y. Matsuo, K. Niikura, and K. Ijiri, *Chem. Commun.*, 2011, **47**, 9426–9428.
8. A. Sánchez-Iglesias, E. Carbó-Argibay, A. Glaria, B. Rodríguez-González, J. Pérez-Juste, I. Pastoriza-Santos, and L. M. Liz-Marzán, *Chem. Eur. J.*, 2010, **16**, 5558–5563.
9. T. A. Taton, C. A. Mirkin, and R. L. Letsinger, *Science*, 2000, **289**, 1757–1760.
10. M. Sakamoto and T. Majima, *Bull. Chem. Soc. Jpn.*, 2010, **83**, 1133–1154.
11. H. Fujita, M. Izawa, and H. Yamazaki, *Nature*, 1962, **196**, 666–667.
12. S. Mosseri, A. Henglein, and E. Janata, *J. Phys. Chem.*, 1989, **93**, 6791–6795.
13. A. Henglein, *Langmuir*, 1999, **15**, 6738–6744.

14. K. Kurihara, J. Kizling, P. Stenius, and J. H. Fendler, *J. Am. Chem. Soc.*, 1983, **105**, 2574–2579.
15. E. Gachard, H. Remita, J. Khatouri, B. Keita, L. Nadjo, and J. Belloni, *New J. Chem.*, 1998, **22**, 1257–1265.
16. A. Henglein and R. Tausch-Tremel, *J. Colloid Interface Sci.*, 1981, **80**, 84–93.
17. B. G. Ershov, E. Janata, and A. Henglein, *Int. J. Radiat. Appl. Instrum. C*, 1992, **39**, 123–126.
18. A. Henglein and D. Meisel, *Langmuir*, 1998, **14**, 7392–7396.
19. P. Mulvaney, M. Giersig, and A. Henglein, *J. Phys. Chem.*, 1993, **97**, 7061–7064.
20. E. Rabinowitch, *Rev. Mod. Phys.*, 1942, **14**, 112–131.
21. Y. Yonezawa, T. Sato, M. Ohno, and H. Hada, *J. Chem. Soc., Faraday Trans. 1*, 1987, **83**, 1559–1567.
22. A. Roucoux, J. Schulz, and H. Patin, *Chem. Rev.*, 2002, **102**, 3757–3778.
23. K. L. McGilvray, M. R. Decan, D. Wang, and J. C. Scaiano, *J. Am. Chem. Soc.*, 2006, **128**, 15980–15981.
24. K. G. Stamplecoskie and J. C. Scaiano, *J. Am. Chem. Soc.*, 2010, **132**, 1825–1827.
25. K. L. McGilvray, C. Fasciani, C. J. Bueno-Alejo, R. Schwartz-Narbonne, and J. C. Scaiano, *Langmuir*, 2012, **28**, 16148–16155.
26. C. M. Gonzalez, Y. Liu, and J. C. Scaiano, *J. Phys. Chem. C*, 2009, **113**, 11861–11867.
27. K. Torigoe and K. Esumi, *Langmuir*, 1992, **8**, 59–63.
28. A. Kameo, A. Suzuki, K. Torigoe, and K. Esumi, *J. Colloid Interface Sci.*, 2001, **241**, 289–292.
29. F. Kim, J. H. Song, and P. Yang, *J. Am. Chem. Soc.*, 2002, **124**, 14316–14317.
30. T. Placido, R. Comparelli, F. Giannici, P. D. Cozzoli, G. Capitani, M. Striccoli, A. Agostiano, and M. L. Curri, *Chem. Mater.*, 2009, **21**, 4192–4202.
31. H. Zeng, X.-W. Du, S. C. Singh, S. A. Kulinich, S. Yang, J. He, and W. Cai, *Adv. Funct. Mater.*, 2012, **22**, 1333–1353.
32. R. Jin, Y. Cao, C. A. Mirkin, K. L. Kelly, G. C. Schatz, and J. G. Zheng, *Science*, 2001, **294**, 1901–1903.
33. C. Xue, G. S. Métraux, J. E. Millstone, and C. A. Mirkin, *J. Am. Chem. Soc.*, 2008, **130**, 8337–8344.
34. J. E. Millstone, S. J. Hurst, G. S. Métraux, J. I. Cutler, and C. A. Mirkin, *Small*, 2009, **5**, 646–664.
35. V. Bastys, I. Pastoriza-Santos, B. Rodríguez-González, R. Vaisnoras, and L. M. Liz-Marzán, *Adv. Funct. Mater.*, 2006, **16**, 766–773.
36. J. Zhou, J. An, B. Tang, S. Xu, Y. Cao, B. Zhao, W. Xu, J. Chang, and J. R. Lombardi, *Langmuir*, 2008, **24**, 10407–10413.
37. B. Pietrobon and V. Kitaev, *Chem. Mater.*, 2008, **20**, 5186–5190.
38. M. R. Langille, J. Zhang, and C. A. Mirkin, *Angew. Chem. Int. Ed.*, 2011, **50**, 3543–3547.
39. J. Zhang, M. R. Langille, and C. A. Mirkin, *Nano Lett.*, 2011, **11**, 2495–2498.
40. C. Xue, J. E. Millstone, S. Li, and C. A. Mirkin, *Angew. Chem. Int. Ed.*, 2007, **46**, 8436–8439.
41. S. Mubeen, J. Lee, N. Singh, S. Krämer, G. D. Stucky, and M. Moskovits, *Nat. Nanotechnol.*, 2013, **8**, 247–251.
42. W. W. Dunn, Y. Aikawa, and A. J. Bard, *J. Am. Chem. Soc.*, 1981, **103**, 6893–6897.
43. A. Takai and P. V. Kamat, *ACS Nano*, 2011, **5**, 7369–7376.
44. P. D. Cozzoli, R. Comparelli, E. Fanizza, M. L. Curri, A. Agostiano, and D. Laub, *J. Am. Chem. Soc.*, 2004, **126**, 3868–3879.
45. C.-T. Dinh, T.-D. Nguyen, F. Kleitz, and T.-O. Do, *ACS Appl. Mater. Interfaces*, 2011, **3**, 2228–2234.
46. N. Zhou, L. Polavarapu, N. Gao, Y. Pan, P. Yuan, Q. Wang, and Q.-H. Xu, *Nanoscale*, 2013, **5**, 4236.
47. L. Carbone, A. Jakab, Y. Khalavka, and C. Sönnichsen, *Nano Lett.*, 2009, **9**, 3710–3714.
48. G. Menagen, J. E. Macdonald, Y. Shemesh, I. Popov, and U. Banin, *J. Am. Chem. Soc.*, 2009, **131**, 17406–17411.
49. X. Li, J. Lian, M. Lin, and Y. Chan, *J. Am. Chem. Soc.*, 2011, **133**, 672–675.
50. M. Quintana, X. Ke, G. Van Tendeloo, M. Meneghetti, C. Bittencourt, and M. Prato, *ACS Nano*, 2010, **4**, 6105–6113.
51. F. B. Lollmahomed and R. Narain, *Langmuir*, 2011, **27**, 12642–12649.
52. G. Moon, H. Kim, Y. Shin, and W. Choi, *RCS Adv.*, 2012, **2**, 2205.
53. V. Tjoa, J. Chua, S. S. Pramana, J. Wei, S. G. Mhaisalkar, and N. Mathews, *ACS Appl. Mater. Interf.*, 2012, **4**, 3447–3452.
54. S. Kirstein, H. von Berlepsch, and C. Böttcher, *Int. J. Photo.*, 2006, **2006**, 1–7.
55. Y. Wei, S. Han, D. A. Walker, S. C. Warren, and B. A. Grzybowski, *Chem. Sci.*, 2012, **3**, 1090–1094.